Authors' Response to Reviews of

The tidal effects in the Finite-volumE Sea ice–Ocean Model (FESOM2.1): a comparison between parameterised tidal mixing and explicit tidal forcing

Pengyang Song et al.
Geosci. Model Dev. Discuss., 10.5194/gmd-2022-25

RC: ***Reviewers' Comment***, AR: Authors' Response, ☐ Manuscript Text

Dear editor and reviewers,

Thanks for the valuable comments on our manuscript. We treat all comments carefully, and list point-to-point responses below. Please also check the revised manuscript with tracked changes.

Yours sincerely,

Pengyang Song et al.

1. Reviewer #1 comments

RC: ***There are some significant improvements in the revised manuscript, but the main problem remains. Over most of the global ocean, the resolution of the model is insufficient to resolve the internal tides. It is therefore obvious from the beginning that the simulation LSTIDE will not capture the increased vertical mixing caused by breaking internal tides. Hence, it is pointless to compare it to CVTIDE, which is constructed to capture precisely this effect. I therefore do not recommend publication.***

Nevertheless, there are some interesting results, in particular the strengthened upwelling in the north Pacific in LSTIDE, and its effect on the global overturning and the hydrography. In the new version it is shown that this is not caused by increased vertical diffusivity K_v , but by increased resolved vertical buoyancy flux $\overline{w'b'}$ in the north Pacific. However, it is still not clear how the tidal motion leads to this buoyancy flux. It is speculated that it is caused by trapped tidal waves at the Kuril–Aleutian Ridge, but no specific support for this is presented. For example, an alternative hypothesis is that propagating internal tides with semidiurnal frequency are involved, since they are in fact resolved in at least part of this region, according to Fig. 15. It should be easy to check this by studying the tidal motion in detail, since the trapped internal tides have diurnal frequency. But even if it shown what kind of tidal waves are involved, it remains to understand why they increase the vertical buoyancy flux.

A manuscript concentrating on these aspects might be publishable. The simulation CVTIDE should then be omitted. It cannot be expected to capture the effect of trapped waves, since its parameterization of the vertical diffusivity is constructed from the scaling of the generation of propagating internal tides.

Such a manuscript would be so vastly different from the present one (with a very different title) that it should be considered as a new submission, not a revised one.

AR: Thank you for your comments. The mixing in the North Pacific is not caused by the semidiurnal internal tides. Because the strength of a baroclinic tide is related to the respective barotropic tide, and the diurnal barotropic tides are much stronger than the semidiurnal ones in the Kuril–Aleutian Ridge (Fig. 1). We can also see from the model output that all signals in the Kuril–Aleutian Ridge show more significant diurnal periods than semidiurnal periods (take one point as an example, Fig. 2).

In our control run, the mesh resolution is eddy-parameterising, and the model has no tides. Thus the model results roughly follow the geostrophic balance. Once we add global tides, we also add ageostrophic flows. Ageostrophic flows, such as tides, can easily cross the isobaths, therefore generating upwelling/downwelling around topographies. That is why LSTIDE increase mixing via turbulent vertical buoyancy flux but not k_v.

We do not agree to delete the CVTIDE part. Because we think comparing LSTIDE with CVTIDE would fill the gap between real tidal mixing and tidal mixing parameterisation. In climate research, a simulation of real tides is not applicable. Thus, improving the parameterisation is the only way to get a better diapycnal mixing in the model. From a climate study's point of view, the comparison is necessary.

RC: ***The language is sometimes incorrect, and needs to be checked. Some corrections are listed below.***

AR: Thank you for the correction. We carefully treated all the comments and some similar grammatical mistakes in our manuscript.

RC: ***There are many lengthy descriptions of figures that add little to what the reader can see for himself. Such descriptions are boring to read, and should be shortened strongly. There are also too many figures. Concentrate on the features that have a clear connection to the main conclusions!***

AR: Thank you for this suggestion. We delete some redundant sentences, figures and tables in the revised manuscript.

RC: ***Page 5, line 128: 'rate of dissipated mechanical energy' should be 'fraction of dissipated mechanical energy'.***

AR: Thank you. This is corrected in the revised manuscript.

RC: ***Page 5, line 144: 'consists with the Prandtl number' should be 'agrees with the Prandtl number'.***

AR: Thank you. This is corrected in the revised manuscript.

RC: ***Page 7, line 207: 'temperature biases' should be 'temperature differences'.***

AR: Thank you. This is corrected in the revised manuscript.

RC: ***Page 9, line 265: 'the depth where the density over depth differs by 0.125 sigma units'. I don't understand this.***

AR: Thank you for pointing out this. To make this clear, we rewrite this sentence as below.

> The second kind of MLD, following Monterey and Levitus (1997), is defined as the depth ~~where the density over depth differs by 0.125 sigma units from the surface density~~ where potential density is higher than the local sea surface density by 0.125 $kg\ m^{-3}$.

RC: ***Page 9, line 279: 'enhanced for 4 Sv' should be 'enhanced by 4 Sv'.***

AR: Thank you. This is corrected in the revised manuscript.

RC: ***Page 9, line 281: 'upwelling for 5 Sv' should be 'upwelling by 5 Sv'.***

AR: Thank you. This is corrected in the revised manuscript.

RC: ***Page 10, line 308: 'surface pressure power' is better described as 'conversion from kinetic energy to***

barotropic potential energy'.

AR: Thank you. This is corrected in the revised manuscript.

RC: ***Page 10, line 310: 'the horizontal distributions show differences', and Page 12, line 356, 'higher buoyancy flux than NOTIDE': According to Fig. 14 h,i the differences are a factor*** 10^{-6} ***smaller than the values for NOTIDE, and hence insignificant.***

AR: Thank you for pointing out this. In the Fig. 14 of the manuscript, panels (g), (h) and (i) are plotted in linear scale, not in decimal logarithmic scale. So the difference is not insignificant. To avoid misunderstanding, we modify this figure (see Fig. 3). The differences in buoyancy flux (Fig. 3b and 3c) are in the same order of magnitude compared with the original values in NOTIDE (Fig. 3a).

However, the new plot does not show consistent positive patterns in the Indonesian Archipelago and Kuril–Aleutian Ridge. Table 1 shows that the regional integrated buoyancy flux in LSTIDE and CVTIDE are stronger than NOTIDE in these two areas. The regional integration results are also added to the revised manuscript.

RC: ***Page 12, line 359 and Fig. 16: Since the buoyancy flux has different sign in different locations, the 'equivalent diffusivity' is negative in many places. Therefore, the interpretation of the buoyancy flux in terms of equivalent diffusivity does not make sense. However, this interpretation is not needed, and can simply be omitted. What matters for the overturning is the diapycnal buoyancy flux, and the importance of the diffusivity is just that it causes such a flux.***

AR: Thank you for this comment. We agree with your suggestion to delete the interpretation of 'equivalent diffusivity'. The turbulent buoyancy flux is shown in Fig. 3. This is corrected in the revised manuscript.

RC: ***Page 12, line 367: 'Trapped internal tides ... can be simulated with LSTIDE'. Check this! Trapped waves have a well defined spatial scale that can be compared to the model resolution, thus extending the analysis in Fig. 15 to the gray areas.***

AR: Thank you for pointing out this. Following Falahat and Nycander (2015), we extend the plot to areas beyond the critical latitudes (Fig. 5). Even though trapped internal tides do not propagate as waves, they are confined in a horizontal scale (Falahat and Nycander, 2015). Figure 5 shows that the mesh applied in this work is fine enough to simulate trapped internal tides in the Kuril–Aleutian Ridge. This explanation is added to the revised manuscript.

Falahat, Saeed, and Jonas Nycander. "On the generation of bottom-trapped internal tides." Journal of Physical Oceanography 45.2 (2015): 526-545.

RC: ***Page 13, lines 391–392: 'the upwelling in the North Pacific and Indonesian Archipelago links to the North Atlantic'. I don't think that this has been shown clearly, even though I agree that the alternative explanation by the Atlantic mixing can be ruled out. If there is such a link, why does it not hold in CVTIDE?***

AR: Thank you for this comment. The linkage between the Indo-Pacific circulation and the Atlantic circulation is the Agulhas Current (Fig. 6). We can find from the barotropic streamfunction difference that there is a connection of the blue pattern between the Indian Ocean and the South Atlantic Ocean in Fig. 6c, but the connection is missing in Fig. 6b. The vector plots of barotropic velocity (around 25° E, 35° S) also show a net transport to the west occurring in Fig. 6c, but to the east in Fig. 6b. The plots indicate that the Agulhas Current is strengthened in LSTIDE but not in CVTIDE, which further alters the strength of the South Atlantic currents and the AMOC. Our results agree with the previous research that the Agulhas leakage has impacts the

MOC (Biastoch et al., 2008). For a better understanding of the cross-basin linkage, we add this explanation to our revised manuscript.

Biastoch, Arne, Claus W. Böning, and J. R. E. Lutjeharms. "Agulhas leakage dynamics affects decadal variability in Atlantic overturning circulation." Nature 456.7221 (2008): 489-492.

RC: ***Page 13, line 395: 'the barotropic streamfunction has an offset effect in the vertical direction'. I don't understand what is meant by this.***

AR: Thank you for pointing out this. To make this clear, we rewrite this sentence as below.

> But note here ~~the barotropic streamfunction has an offset effect in the vertical direction~~ the vertical structure of oceanic circulation cannot be revealed by the barotropic streamfunction .

RC: ***Page 16, lines 481–482: The text seems to indicate that the increased ITF is caused by the increased upwelling in the north Pacific. A similar impression is given on page 12, line 362. However, the connection has not been shown. Perhaps the increased ITF is mainly caused by increased buoyancy flux and upwelling in the Indonesian Archipelago?***

AR: Thank you for this comment. The streamfunction in the Fig. 11f of the manuscript shows the two upwelling regions in LSTIDE: the Kuril–Aleutian Ridge and the Indonesian Archipelago. Focusing on the upper 2000 m of the plot, we can find that the increase of ITF comes from both local (Indonesian Archipelago) upwelling and remote (Kuril–Aleutian Ridge) upwelling. By roughly estimating from the Fig. 11f of the manuscript, half of the increased ITF originates from the North Pacific cell, and the other half belongs to the South Indo-Pacific cell. Thus, the increased ITF is not only caused by the upwelling in the North Pacific. To avoid this misunderstanding, we revise the sentence as below.

> Our results show that the tidal mixing in these two areas drives stronger upwelling in the deep Pacific Ocean. In the Kuril–Aleutian Ridge, deep water is upwelled to the intermediate layer and advected to the tropical region; in the Indonesian Archipelago, ~~the upwelled deep water enhances the ITF along with the intermediate water from the north~~ deep water is also upwelled to the intermediate layer and advected to the further south. Both upwelled water contributes to the ITF enhancement .
>
> The strong mixing upwells an additional 5 Sv of deep water in the North Pacific (around 50° N) to the intermediate layer and then spreads to the south (Fig. 11f). ~~The intermediate water then contributes to the ITF (Fig. 13c) and flows into the Indian Ocean~~ The strong mixing in the Indonesian Archipelago also results in strong upwelling. The upwelled water from both the Indonesian Archipelago and Kuril–Aleutian Ridge contributes to the ITF (Fig. 13c) and flows into the Indian Ocean .

RC: ***Figure 12: The units of the color scales should be given. It is also very unclear to me what is meant by 'difference of scaled vertical diffusivity'. It is strange that the differences seem to be several orders of magnitude larger than the values in NOTIDE.***

AR: Thank you for pointing out this. What we wanted to show is that the deep-ocean vertical diffusivity in CVTIDE is one to two orders larger than NOTIDE.

This is true in the model. In NOTIDE, the KPP scheme provides a background vertical diffusivity of $10^{-5}m^2s^{-1}$, and the shear-induced diffusivity is small due to the low velocity in the deep ocean. In CVTIDE, the deep-ocean vertical diffusivity contains an additional component from the CVMIX_TIDAL parameterisation, which provides a vertical diffusivity up to $0.5 \times 10^{-2}m^2s^{-1}$. Comparing the two values, one can find that the vertical diffusivity in CVTIDE is at most three orders of magnitude larger than the values in NOTIDE. But if we calculate the global average, this difference is about one order of magnitude, as shown by Simmons et al. (2004). Since tidal mixing is bottom-enhanced, we change the approach to show the vertical diffusivity, and the plot is modified as Fig. 7.

Simmons, Harper L., et al. "Tidally driven mixing in a numerical model of the ocean general circulation." Ocean Modelling 6.3-4 (2004): 245-263.

RC: ***Figure 14: The units of the color scales should be given. The sign of the buoyancy flux seems mostly positive in the plots, which contradicts the negative value in Table 3. Does the viscous dissipation include both horizontal and vertical viscosity?***

AR: Thank you for pointing out this. To avoid misunderstanding, we leave the decimal logarithmic scale only in the colorbars. Also, the units are given in the plots.

Besides, we found two mistakes in our plotting routine. One mistake is that we used natural logarithms (log) instead of decimal logarithms (log10), that causes the errors in plotting the bottom drag and viscous dissipation. The second mistake is that we used filled contour plots (tricontourf) instead of pseudocolor plots (tripcolor). Filled contour plots seem to overlook the scattered patterns, which is why there seem to be no negative values in the Figs. 14h and 14i of the manuscript.

In the Figs. 14d, 14e and 14f of the manuscript, we plotted only vertical viscous dissipation. Since horizontal viscous dissipation is diagnosed in our manuscript, the revised figure includes both horizontal and vertical viscous dissipation. We mention this in our revised manuscript.

To sum up, the Fig. 14 of the manuscript is revised as Fig. 3 and Fig. 4 below.

RC: ***Figure 15: Give the explicit expression for the plotted ratio.***

AR: Thank you for this comment. Explicit expressions are added to the revised manuscript.

2. Reviewer #2 comments

RC: ***Upon request from the topical editor, the revised version of the manuscript has been reviewed in view of the interactive public discussion. I should report on this assessment. In the light of a criteria whether the authors responded appropriately to the reviewers' original concerns or not, I think that the authors have made a basically good response. But I think some additional work is required before the paper can be accepted for final publication.***

AR: Thank you for your comments. Point-to-point responses are listed below.

RC: ***The second comment of Reviewer #1 and the first comment of Reviewer #2 commonly concern the reality of the sink for the long internal tidal waves in LSTIDE experiment with explicit tides. Authors seems to have reached a conclusion that the convergence of vertical turbulent buoyancy flux due to tides balances the vertical advection term for the mean field, contrary to their first thought that the vertical mixing in LSTIDE experiment would be enhanced by vertical shear of baroclinic tides. This may not be realistic as the reviewers have pointed out, but would be reasonable given the spatial resolution of the model being used here. I think the novelty and value of this paper is to have presented how the meridional overturning circulations would change in a simulation with explicit tides. For the paper to set a useful basis for future works with high-resolution models and to have a lasting value, two-dimensional map of energy sink for***

LSTIDE experiment should be desirably compared with one of state-of-the-science estimates such as the one presented by de Lavergne et al. (2019) and differences are discussed.

AR: Thank you for this comment. Comparing results from a tide model with de Lavergne et al. (2019) would be interesting, but we think it is unnecessary for this work. The low-resolution mesh we applied is for climate simulations, thus (1) the model does not generate enough baroclinic tidal energy; (2) the model cannot describe high-mode internal tides; (3) the model cannot simulate wave-wave interactions. Such comparison can only be made by using a much higher resolution, such as 0.1° (Li et al., 2015), but then we cannot simulate a long-term ocean state due to the limitation of computational capacity. We agree that some work on comparing simulation and theoretical results would be valuable, but not much related to our focus.

de Lavergne, Casimir, et al. "Toward global maps of internal tide energy sinks." Ocean Modelling 137 (2019): 52-75.

Li, Zhuhua, Jin-Song Von Storch, and Malte Müller. "The M2 internal tide simulated by a 1/10° OGCM." Journal of Physical Oceanography 45.12 (2015): 3119-3135.

RC: ***The globally integrated kinetic energy budget for the three experiments is presented in Table 3. The value for the buoyancy flux term is the same for all experiments. I think more explanation for this feature would be useful.***

AR: Thank you for mentioning this. The values of global integration are close, but not identical (because only the first two decimal places are kept). We add regional integration results in Table 1. By integrating over the Kuril–Aleutian Ridge (120° E–120° W, 30° N–60° N) and Indonesian Archipelago (90° E–150° W, 15° S–15° N), we can see that the values of regional integration are different. Note here negative values indicate upwelling. For comparison, we also give the values of regional integration over the North Atlantic (60° W–10° E, 45° N–70° N), which are positive values. It is also comprehensible that LSTIDE shows larger positive values in the North Atlantic due to the stronger AMOC.

RC: ***What is the source of the temporal mean square tidal velocity distribution used for CVTIDE experiment? How different are the distribution used for CVTIDE and that of LSTIDE? Or are they common?***

AR: Thank you for this comment. The forcing file used in CVTIDE is interpolated from the file used in Jayne (2009), originating from Jayne and St. Laurent (2001). The forcing file only consists of energy dissipation, which is calculated via Eq. (3) in the manuscript. We cannot find the original temporal mean square tidal velocity distribution from the file.

However, to our knowledge, the tidal model Jayne (2009) used is driven by the largest eight tidal components. In LSTIDE, we use the lunisolar gravitational potential, which consists of all tidal components theoretically. But note that except for the largest eight tidal components, the rest tidal constituents are minor.

Since we do not have the output from the tidal model of Jayne (2009), we cannot directly compare. But we assume both tidal models are valid, so the temporal mean square tidal velocity distribution should be close. The validation of the tidal potential module in our work is shown in Section 3.

Jayne, Steven R., and Louis C. St. Laurent. "Parameterizing tidal dissipation over rough topography." Geophysical Research Letters 28.5 (2001): 811-814.

Jayne, Steven R. "The impact of abyssal mixing parameterizations in an ocean general circulation model." Journal of Physical Oceanography 39.7 (2009): 1756-1775.

Table 1: Regional integrated buoyancy flux in three typical areas. Buoyancy flux is expressed as $\rho_0 bw$.

Experiment ID	Kuril–Aleutian Ridge	Indonesian Archipelago	North Atlantic
NOTIDE	-1.22	-0.82	0.38
CVTIDE	-1.52	-1.13	0.39
LSTIDE	-2.78	-1.19	0.49

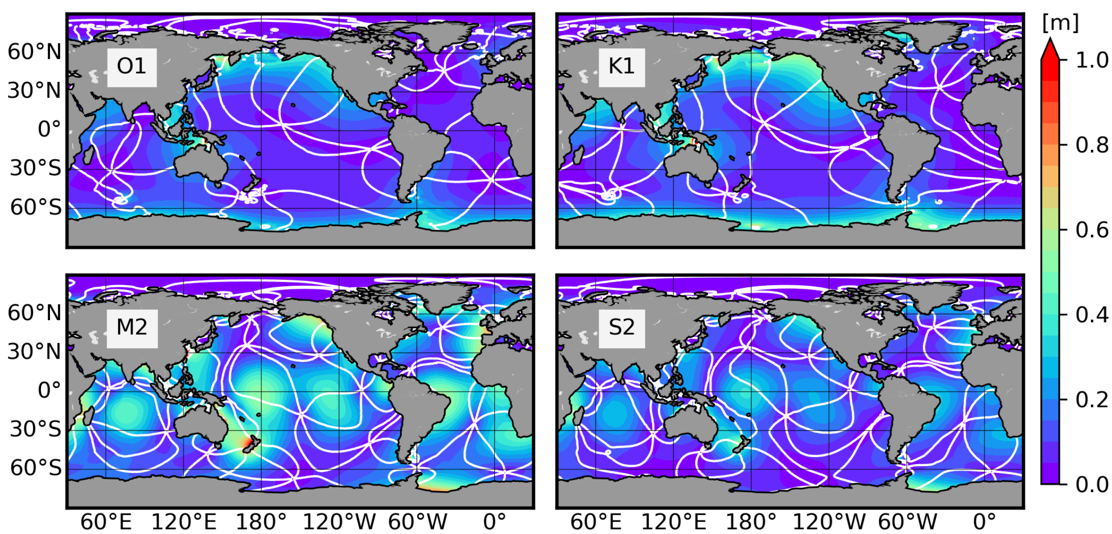

Figure 1: Co-tidal charts of the four main tidal components from the tide model. The colours indicate tide amplitudes, and the white lines indicate Greenwich phase lags with an interval of 60°.

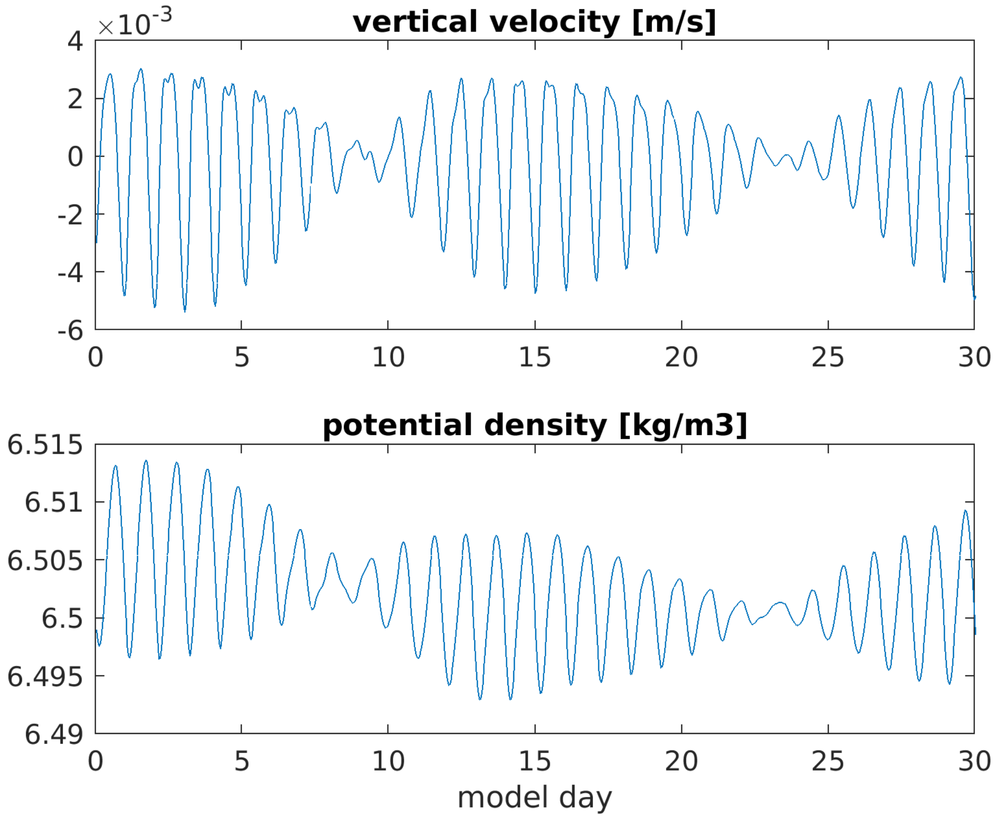

Figure 2: Vertical velocity (w) and potential density (ρ) from one-point hourly-output results. The model point locates at 1920 m in 165° E, 55° N. Potential density is model potential density minus a constant value (1030 kg/m^3).

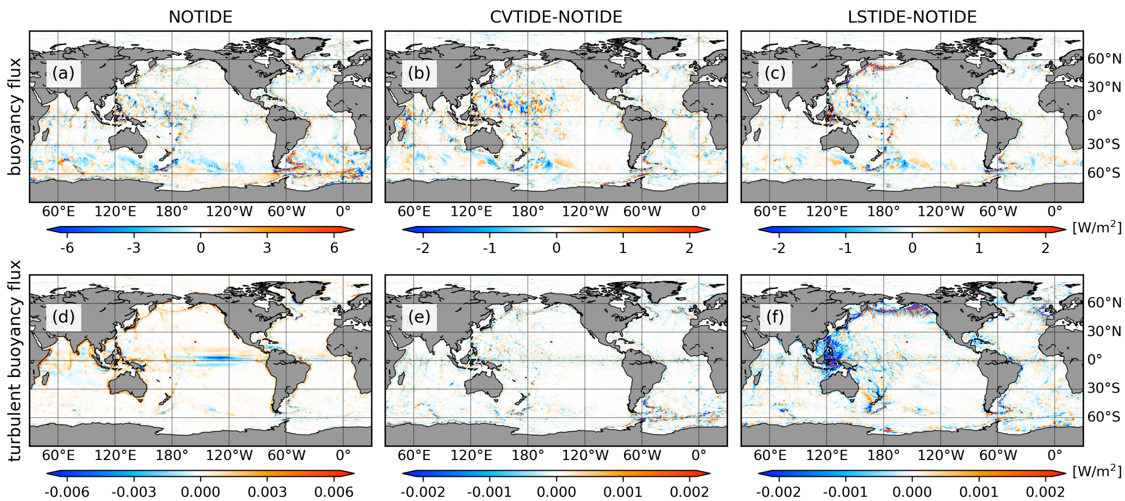

Figure 3: Horizontal distribution of vertically integrated buoyancy flux terms. Buoyancy flux is expressed as $g\rho w$, while turbulent buoyancy flux is $\overline{g\rho' w'}$ (positive values represent upwelling). The left column shows the control run, and the middle and right columns show the differences.

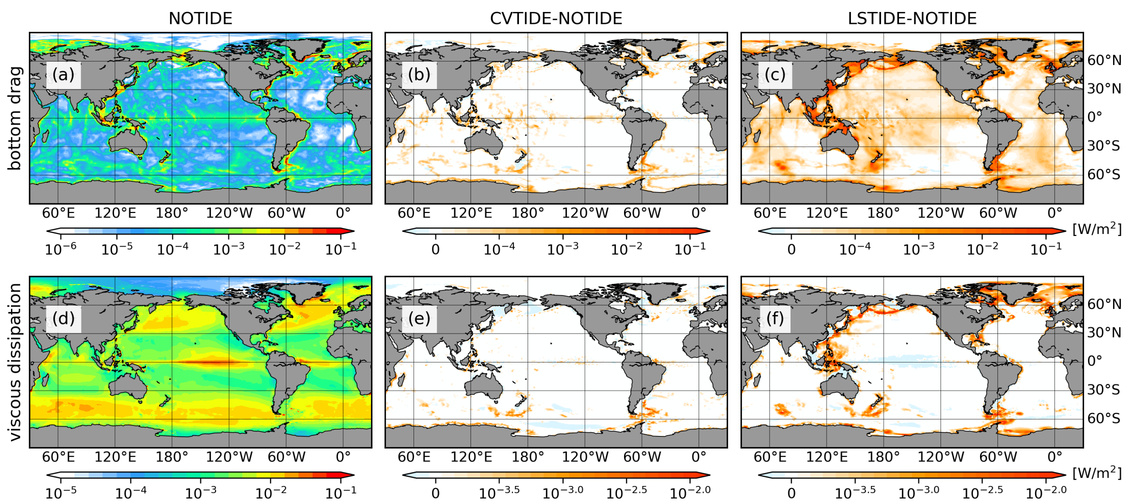

Figure 4: Horizontal distribution of vertically integrated energy dissipation terms in Table 3 of the manuscript (positive values represent energy dissipation). The upper and lower rows indicate bottom drag and viscous dissipation (including horizontal and vertical components). The left column shows the control run, and the middle and right columns show the differences. Note that the plots are shown in a decimal logarithmic scale.

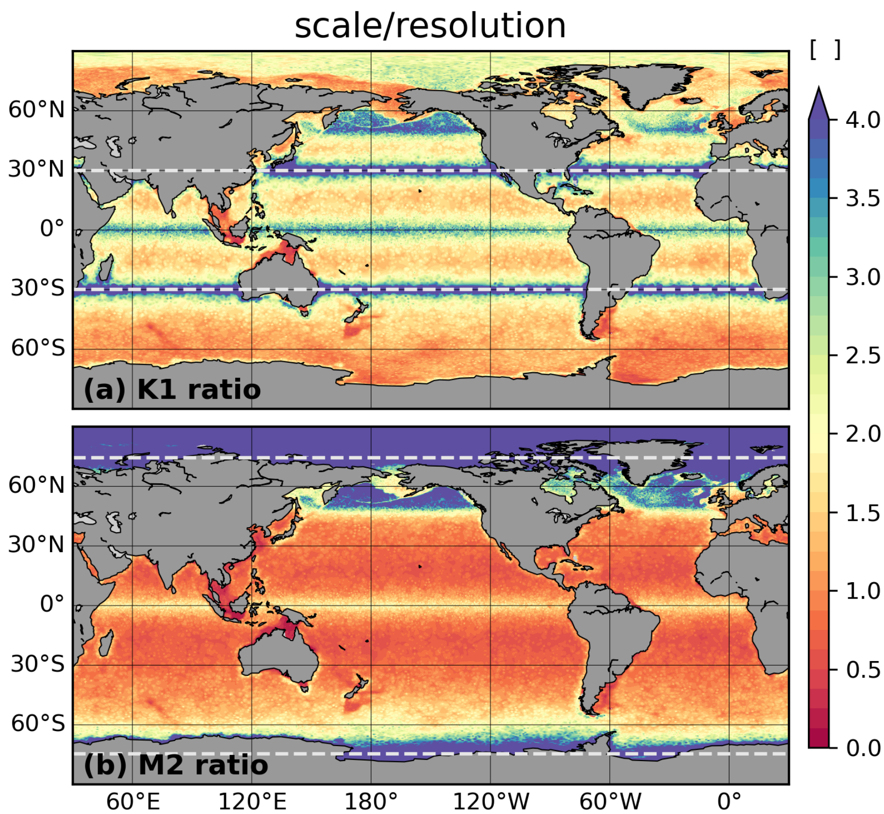

Figure 5: The ratio of mode-1 K1/M2 internal tide scale and mesh resolution. The thick grey dashed line indicates the critical latitudes of internal tides.

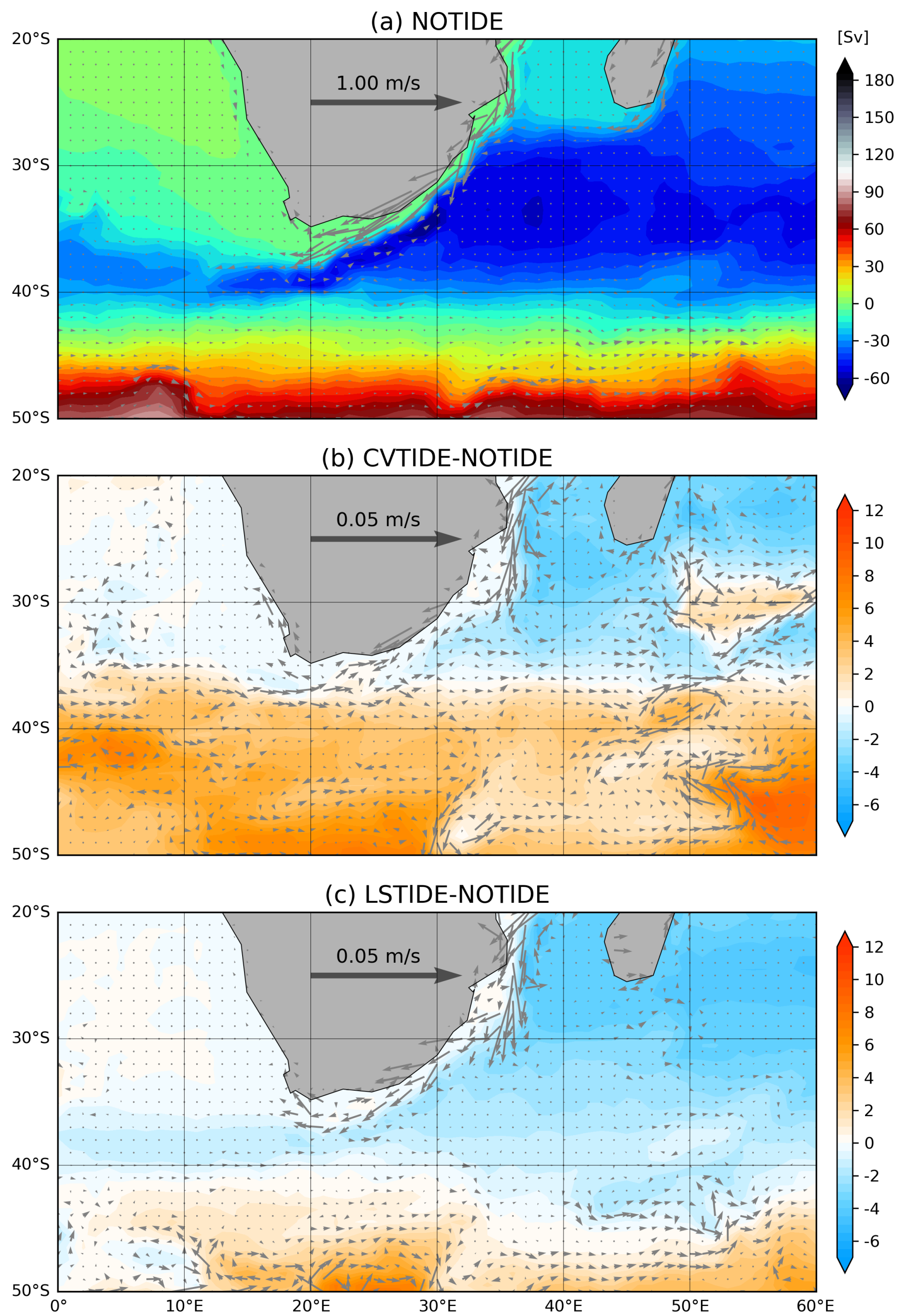

Figure 6: The barotropic streamfunction and velocity in the three sensitivity runs. The shading plot shows the barotropic streamfunction, which is the same as Figure 13 in the manuscript but zoom in the Agulhas current region. The vector plot shows the barotropic velocity. The upper panel shows the control run, while the middle and lower panels show the differences.

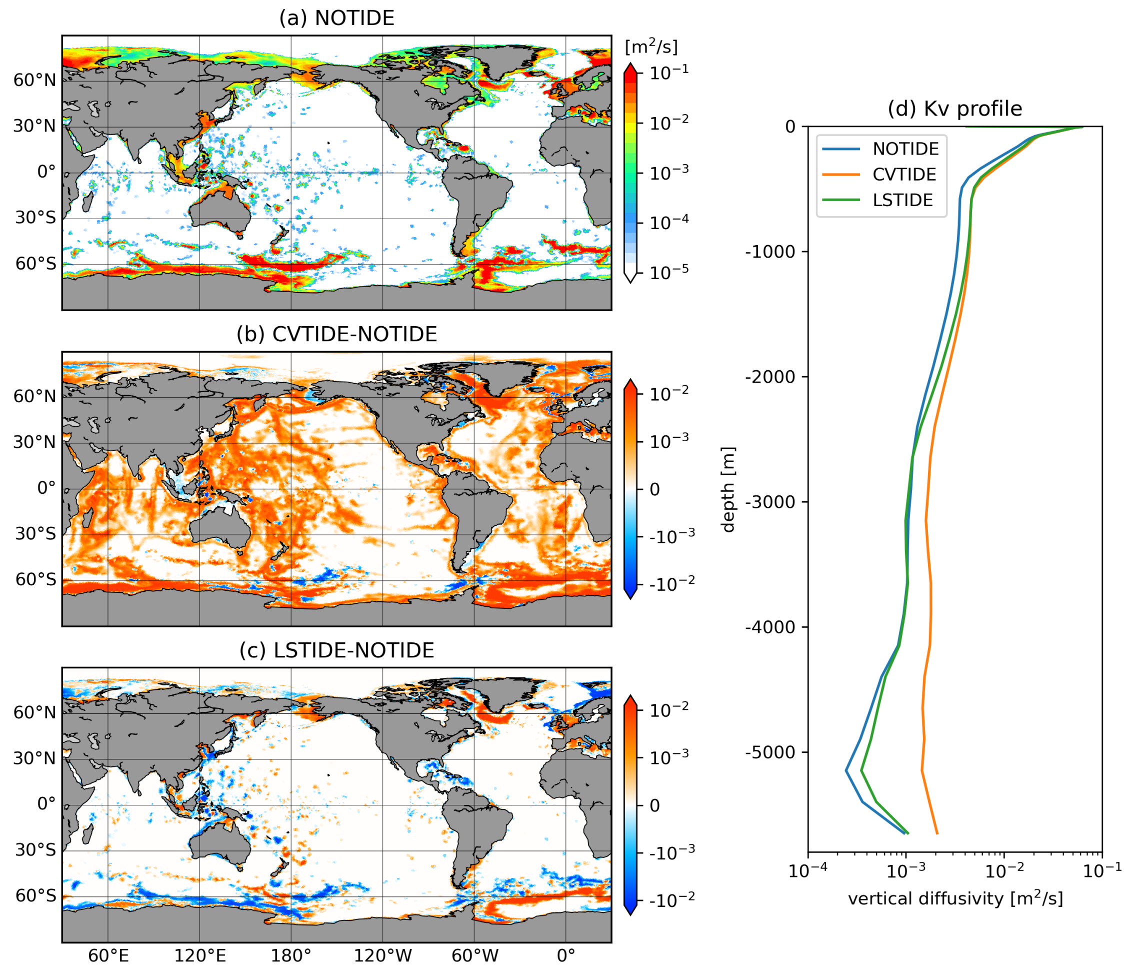

Figure 7: The left panels are horizontal maps of depth-averaged vertical diffusivity over the bottom 500 m (average over the whole depth where bathymetry is less than 500 m). The right panel shows the global mean vertical diffusivity profile in the three sensitivity runs. Note that colorbars are shown in decimal logarithmic scales.